

LETTER

## A novel anode structure for diffuse arc anode attachment

To cite this article: Ya-Hao Hu *et al* 2021 *J. Phys. D: Appl. Phys.* **54** 36LT01

View the [article online](#) for updates and enhancements.

### You may also like

- [Investigation of the relationship between arc-anode attachment mode and anode temperature for nickel nanoparticle production by a DC arc discharge](#)  
Feng Liang, Manabu Tanaka, Sooseok Choi *et al.*
- [Comparative analysis of the arc characteristics inside the converging-diverging and cylindrical plasma torches](#)  
Jianghong SUN, , Surong SUN *et al.*
- [Using arc voltage to locate the anode attachment in plasma arc cutting](#)  
D J Osterhouse, J W Lindsay and J V R Heberlein



## ECS Membership = Connection

### ECS membership connects you to the electrochemical community:

- Facilitate your research and discovery through ECS meetings which convene scientists from around the world;
- Access professional support through your lifetime career;
- Open up mentorship opportunities across the stages of your career;
- Build relationships that nurture partnership, teamwork—and success!



**Join ECS!**

**Visit [electrochem.org/join](https://electrochem.org/join)**



## Letter

# A novel anode structure for diffuse arc anode attachment

Ya-Hao Hu<sup>1,2</sup>, Xian Meng<sup>2</sup>, He-Ji Huang<sup>2</sup>, Anthony B Murphy<sup>3</sup> , Ke Shao<sup>1,2</sup>, Su-Rong Sun<sup>1,\*</sup> and Hai-Xing Wang<sup>1,\*</sup> 

<sup>1</sup> School of Astronautics, Beihang University, 100191 Beijing, People's Republic of China

<sup>2</sup> Institute of Mechanics, Chinese Academy of Sciences, Beijing, 100190 Beijing, People's Republic of China

<sup>3</sup> CSIRO Manufacturing, PO Box 218, Lindfield, NSW 2070, Australia

E-mail: [ssr18@buaa.edu.cn](mailto:ssr18@buaa.edu.cn) and [whx@buaa.edu.cn](mailto:whx@buaa.edu.cn)

Received 11 March 2021, revised 2 June 2021

Accepted for publication 14 June 2021

Published 24 June 2021



CrossMark

### Abstract

A novel method for adjusting the direct current arc anode attachment mode by changing the anode surface structure is proposed. A transferred arc device is used to investigate the effect on the arc anode attachment state of the electrode separation and the presence and dimensions of an annular boss, or embossing, on the anode. The experimental results show the diffuse arc anode attachment mode is more likely to be formed in the presence of an annular boss structure on the anode, compared to the standard planar structure. In the case of argon working gas, as the distance between the cathode and the anode increases from 15 mm to 30 mm, the arc maintains the diffuse arc attachment on the anode with the annular boss, while for a planar anode, the arc anode attachment mode changes from diffuse to constricted. Comparison of the measured temperature distribution by the relative intensity method and the emission intensity of the arc attachment region verifies that the annular boss anode can indeed promote diffuse attachment. Analysis of the electric field strength distribution between the electrodes shows that the introduction of the annular boss doubles the electric field strength near the anode surface due to the boss edge effect, which drives the arc to be evenly dispersed on the boss, resulting in the formation of diffuse arc attachment. The enlarged attachment area reduces the current density and heat flux on the anode surface, which is important for the stabilization of diffuse arc attachment. No obvious ablation is found on the surface of the annular boss anode after 1 h operation, while there significant ablation is evident on the surface of the planar anode.

**Keywords:** Arc anode attachment, diffuse arc attachment, anode structure, emission spectroscopy, electrode erosion, transferred arc, thermal plasma

(Some figures may appear in colour only in the online journal)

### 1. Introduction

Direct current (DC) arc plasma devices are widely used as high-temperature heat sources in material processing, aerospace, and waste treatment [1]. In these devices, the arc

anode attachment mode directly determines the heat flux distribution on the anode surface and therefore affects the performance and service life of the arc plasma device. Arc anode attachment modes have consequently been the subject of many studies. Previous experimental observations and theoretical analysis have shown that the arc anode attachment mode can be divided into the diffuse mode, the constricted mode, the multi-arc root attachment and other transitional attachment

\* Authors to whom any correspondence should be addressed.

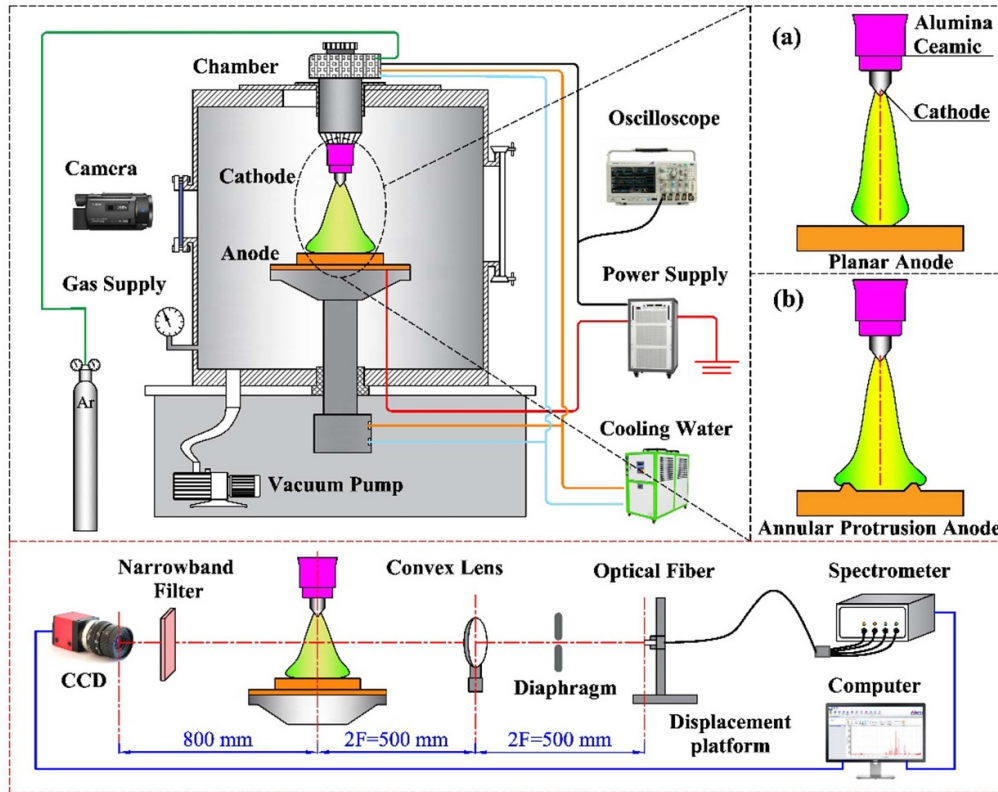


**Figure 1.** Schematic of experimental setup to observe the arc anode attachment.

modes [2–8]. Among these, the constricted arc anode attachment often leads to the extremely high current and heat flux density on the anode surface, so that the arc attachment region is often subjected to strong ablation when there is insufficient anode cooling [9–12]. Although some methods and measures, such as external magnetic field rotating arc [13], gas-dynamic dispersion [14, 15] and multi-electrode structure [16], have been introduced in attempts to modify the attachment mode, there is still ample room for improvement.

It is well known that the electrode's surface morphology, such as tiny bumps, burrs, roughness, etc, can affect the interaction between the arc and the electrode. Since the micro-scale structure of the cathode, such as micro-protrusions, is closely related to the emission properties and arc ignition, intensive studies of this issue have been performed for vacuum arcs [17–19]. It is found that the presence of such micro-scale structure on the electrode surface leads to the enhancement of the local electric field of the electrode. The enhancement of the field strength of a surface can be described by the ad hoc introduction of a field enhancement factor  $\beta$ , which is the ratio of the actual field strength with micro-protrusion and the ideal field strength for a smooth electrode surface. For the cathode, the electric field enhancement coefficient may exceed 100, or even 1000 in some cases, which has a significant influence on the emission properties of the cathode [20]. Micro-scale structures also occur on the anode surface for various reasons. Even for a smooth anode surface, the arc interacts with the anode surface to cause roughness on the order of nanometres

to micrometres during the operation of the arc device. When the anode is severely ablated, cavities of the order of millimetres or more may be formed. This kind of anode micro-scale structure, in particular the resulting micro-protrusions, has a great influence on arc anode attachment. It is usually found in experiments that the arc tends to attach to locations with protrusions. The influence of the micro-protrusions on the arc anode attachment is expected to be related to the enhancement of the electric field on the anode surface caused by the micro-protrusions.

Here we look at this issue from a different point of view. We ask whether, since the micro-protrusions on the anode surface can affect the arc anode attachment, it is possible to adjust the arc anode attachment by artificially providing a regular protruding structure on the electrode? To examine the question, we produced an annular boss (an annular protrusion or embossing) on the anode surface and used an argon transferred arc, as shown in figure 1, to investigate the effect of anode surface structure on the arc attachment.

## 2. Experimental setup

In the experiment, the electrode arrangements of the transferred arc device are shown on the right side of figure 1. The device includes a thoriated tungsten cathode with a diameter of 5 mm and a 60-degree cone angle at the tip, and a copper anode that is perpendicular to the cathode axis. An IGBT

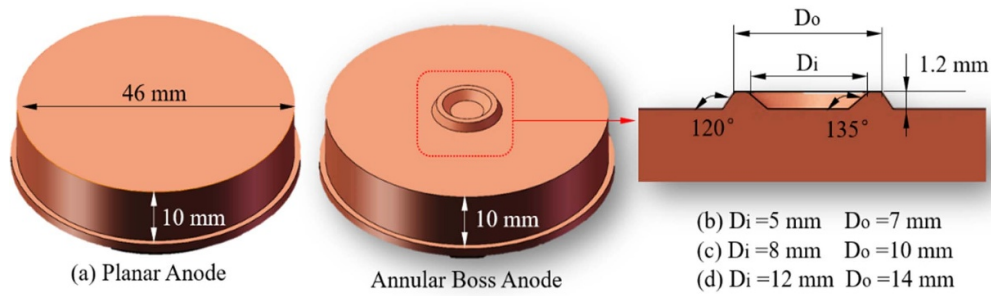


**Figure 2.** The structure and dimensions of the annular boss used in the experiment.

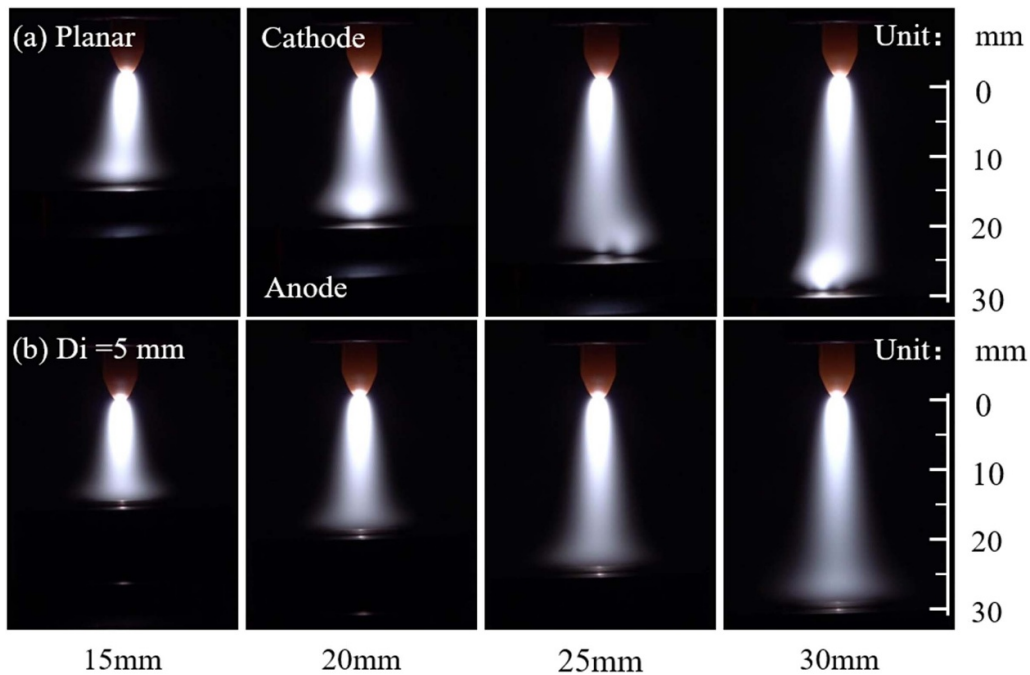


**Figure 3.** Comparison of arc anode attachments with changing electrode separation, group (a) planar anode and group (b) annular boss anode.

inverter DC constant current power supply that can provide currents from 40 to 160 A was used. The arc current is 60 A. The working gas is supplied through the channel between the cathode and the alumina ceramic cover, with a flow rate of 10 standard litre per minute (slm). A four-channel spectrometer (AvaSpec-ULS4096CL) with an optical fibre (200  $\mu\text{m}$ ) fixed on a displacement platform (with an accuracy of 0.001 mm) was adopted to record the radial distribution of emission intensity. The images of argon arc were recorded by a CCD with two narrow-band filters, with a bandwidth of 10 nm, at wavelengths 675.28 nm and 696.54 nm, respectively. An anode with an annular boss and a carefully polished planar anode are respectively used to conduct a comparative observation experiment of arc anode attachment. The two kinds anodes have the same thickness of 10 mm, the same overall diameter of 46 mm and the same water cooling conditions are used for each anode. The structure and dimensions of the annular boss anode used in the experiment are shown in figure 2.

### 3. Results and discussion

Figure 3 shows photos of the arc attachment to the anode for different electrode separations. The arc photos were taken by a Sony FDR-AX700 camera with a pixel resolution of  $421 \times 561$ , using an exposure time of 100  $\mu\text{s}$ . A Vario-Sonnar T\* camera lens with an f/11 aperture was used, together with a neutral density filter (ND 0.6). It can be clearly seen from figure 3(a) that for the annular boss anode, as the electrode spacing increases from 15 mm to 30 mm, a relatively stable diffuse arc attachment mode is maintained on the anode surface. For the planar anode shown in figure 3(b), it can be seen that with the increasing electrode separation, the arc attachment mode changes from the diffuse to constricted, then multi-point, and finally, a more intensely constricted attachment that deviates significantly from the arc axis. The arc voltage increases significantly with the electrode separation for both planar and annular boss anodes. However, there is

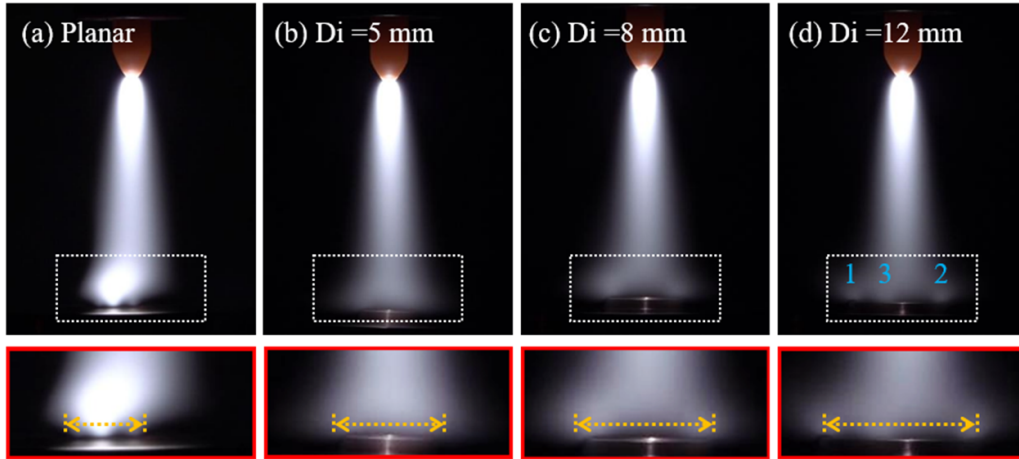


**Figure 4.** Comparison of arc anode attachment with the difference anode structure (a) planar anode, (b)–(d) annular boss anode with different boss diameters.

little difference between the arc voltage for the planar and annular boss anodes for the same interelectrode gap.

To further study the effect of the annular boss on the arc anode attachment, we kept the electrode separation (30 mm) and the operating parameters unchanged to examine the effects of the diameter of the annular boss. To facilitate comparison, figure 4(a) shows the experimental photo of arc attachment at the planar anode, while figures 4(b)–(d) present photos of arc attachment for three annular boss diameters. It should be noted that we kept the shooting conditions consistent in order to make the photos of different anodes comparable. Saturation occurs in the arc centre near the planar anode in figure 4(a), but it does not affect the analysis of the results or the conclusions. It can be seen that, compared with the planar anode, all the annular boss anodes with different sizes have a significant dispersing effect on the arc anode attachment. However, it can also be observed from figure 4 that when the size of the annular boss is larger, the arc attaching to the anode tends to be multiple points. Therefore, it can be predicted that when the diameter of the annular boss is larger than a certain value, the dispersing effect of the annular boss on the arc attachment decreases. For larger diameters, the attachment tends to be consistent with the arc attachment on the planar anode.

Based on the photos given in figure 4, the effects of different anode structure on the arc anode attachment can be further analyzed. We can set a specific grey value from the photo to represent the width of the arc attachment to the anode. Here, the grey value of 51 (20% of the maximum grey value 255) at 2 mm above the lowest part of the anode is defined as the boundary threshold of the arc attachment region. The widths of the arc attachment region calculated based on this method are shown in the lower part of figure 4. Because the temperature of the arc is positively correlated with the brightness of the image (below the maximum emission of argon lines), the average temperature of the arc attachment region corresponding to different anode types can also be compared semi-quantitatively using the sizes of average grey value within the arc attachment range. They are obtained by averaging the grey values of all pixels within the arc width determined by the grey boundary

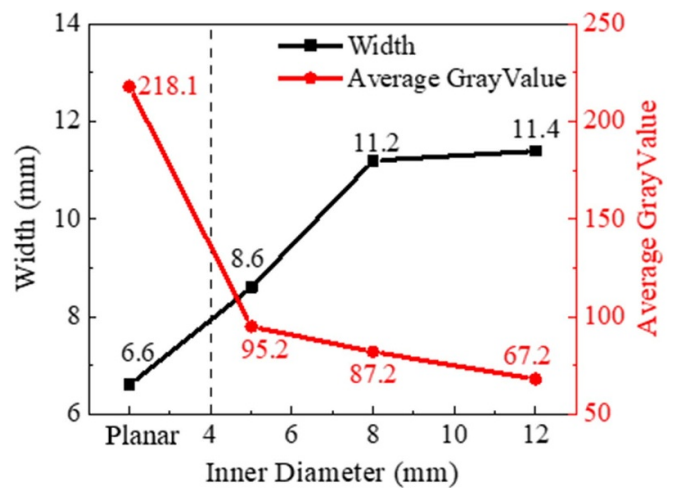


**Figure 5.** Comparison of the width and average grey value of the arc attachment at 2 mm above the lowest part of the surface for different anode types (a) planar anode, (b)–(d) annular boss anode with different bosses.

threshold. Figure 5 presents the arc anode attachment width and the average greyscale of the arc attachment region for the different anode types obtained based on the experimental photos of figure 4.

It can be seen from figure 5 that the arc anode attachment width is the smallest, and the brightness is the highest, for the planar anode. For the anodes with an annular boss, as the diameter of the annular boss increases, the width of the arc anode attachment increases, and the brightness gradually decreases. The results demonstrate that the annular boss has a significant dispersing effect on the arc anode attachment. It is noted from figure 5 that the arc width rises significantly, i.e. from 8.6 to 11.2 mm, when the inner diameter of annular boss anode increases from 5 mm to 8 mm, while the increase in the arc width at the anode attachment site is not obvious when the inner diameter of annular boss anode increases from 8 mm to 12 mm.

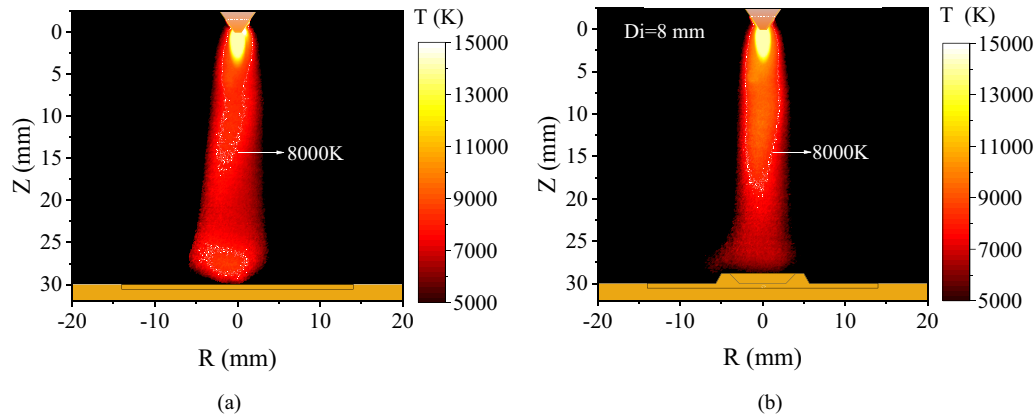


**Figure 6.** Arc temperature distribution for planar (a) and annular boss with inner diameter 8 mm and outer diameter 10 mm (b) anodes measured by relative intensity method of emission spectroscopy.

Temperature distributions of the transferred arc are given in figure 6 for the different anode structures. The arc temperature measurement method is based on the relative intensity method of the emission spectrum which is described in [21–23]. The method is based on arc image processing technology and the relative intensity ratio of two specific spectral lines. The grey images of the arc were taken by the CCD camera through two narrow-band filters with central wavelengths of 675.28 nm and 696.54 nm, respectively. The arc was stable, and the shooting conditions were identical. Therefore, the images taken by the CCD at different times for the two filters could be superimposed. The radial distributions of emission intensity of the 675.28 and 696.54 nm Ar I lines were obtained by scanning the spectrum along the radial direction with the displacement platform. By calibrating the emission intensity with the grey value at the corresponding positions, one can establish the relationship between emission intensity and grey value. The grey values recorded by the CCD with different narrow-band filters can then be converted to the temperature distributions of the arc plasma. In this study, the temperature distributions are not obtained from spatial reconstructed by Abel-inversion. They are calculated by the emission superimposed along the line of sight, which is actually a method to obtain the averaged parameters of the line-of-sight. For more details of the calibration process and the relative intensity calculation of the two spectral lines to obtain the temperature distribution, refer to [21–23].

It can be seen from figure 6 that, in the case of a planar anode, the arc anode attachment is in a constricted mode. In addition to a high-temperature zone adjacent to the cathode, the arc also forms a zone of relatively high temperature, which can reach 7000–8000 K, above the surface of the anode due to the constriction of the arc. However, in the case of an annular boss anode, the arc temperature decreases monotonically along the central axis from the high-temperature region below the cathode to the anode surface. It shows that for the annular boss anode, there is no high-temperature zone caused by arc constriction at the arc anode attachment region. It should keep in mind that there are some limitations in the accuracy of temperature measurement methods used in

this study. The relative intensity method of emission spectra is based on the assumption of local thermodynamic equilibrium (LTE). For the arc fringes and the electrode attachment regions, the plasma deviates from LTE, and the measurement results lose accuracy. Nevertheless, the measured temperature distributions present a reasonable comparison of the relative states of arc anode attachment for the two anode structures. In particular, it should be noted that the differences in temperature persist up to more than 5 mm above the anode, and deviations from LTE are only expected within 1 mm of the anode.

The electrostatic field distributions, calculated in a two-dimensional axisymmetric ( $r$ - $z$ ) coordinate system, for planar (a) and annular boss (b) anodes are shown in figure 7. The voltage between the anode and the cathode is set to 25 V, which is of the same order as the arc voltage for the argon transferred arc with arc current of 60 A and gas flow rate of 10 slm. It can be seen from figure 7 that for the planar anode, the electric field strength distribution on the anode surface is relatively uniform. In contrast, for the annular boss anode, the electric field strength near the annular boss is obviously enhanced.

Figure 8 further shows a comparison of the radial distribution of the electric field strength 1.25 mm above the lowest part of the anode for the planar and the annular boss anodes. It can be clearly seen from figure 8 that, due to the change of the structure of the anode, the electric field strength near the annular boss is substantially larger than that of the planar anode. The electric field strength has a clear ‘M-shaped’ distribution on each side of the annular boss anode. The two peaks occur at the edges of the annular boss, with the larger value of  $700 \text{ V m}^{-1}$  occurring near the outer edge and the inner edge value being  $650 \text{ V m}^{-1}$ . This is because the outer edge angle  $120^\circ$  is smaller than the inner edge angle  $135^\circ$  for the annular boss anode, thus resulting in a stronger electric field at the outer edge. In the central part of the ‘M-shaped’ peaks, corresponding to the flat top of the annular boss, the electric field strength is about  $500 \text{ V m}^{-1}$ , which is much lower than the electric field strength on the boss edges. This means that the edges, rather than the flat part of the annular boss, make the

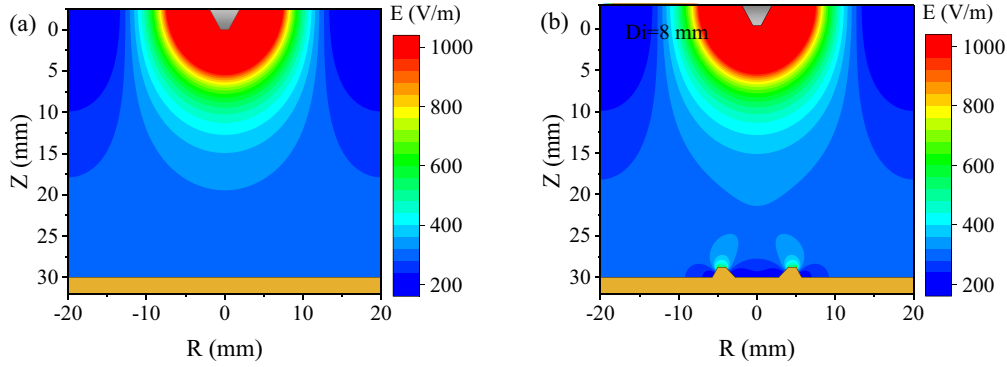


**Figure 7.** The calculated electric field strength distributions for planar (a) and annular boss with inner diameter 8 mm and outer diameter 10 mm (b) anodes.

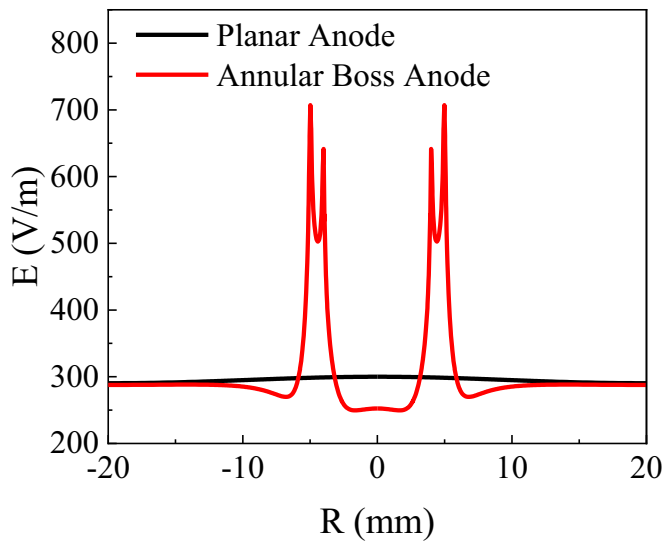


**Figure 8.** The calculated radial distribution of electric field strength 1.25 mm above the lowest part of the surface for planar and annular boss anodes.

main contribution to the electric field strength enhancement. According to the definition of the electric field enhancement coefficient  $\beta$  discussed above,  $\beta$  for this annular boss structure is  $\sim 2$ . The change of electric field strength changes the current density distribution of the arc anode, thereby affecting the distribution of the Lorentz force on the anode surface. According to a previous analysis [7], the main reason for the formation of the constricted arc attachment mode is a relatively high current density at the anode attachment region, which leads to anode jet formation via the Lorentz force, which is due to the interaction of the current with the self-induced magnetic field. The annular boss enhances the electric field, causing the arc to be evenly distributed on the boss, which increases the arc anode attachment area and decreases the current density, thereby preventing the formation of an anode jet. Although this enhancement factor is much smaller than the magnitude of the electric field enhancement factor caused by some micro-scale structures on the cathode surface, it is sufficient to change the arc anode attachment state.

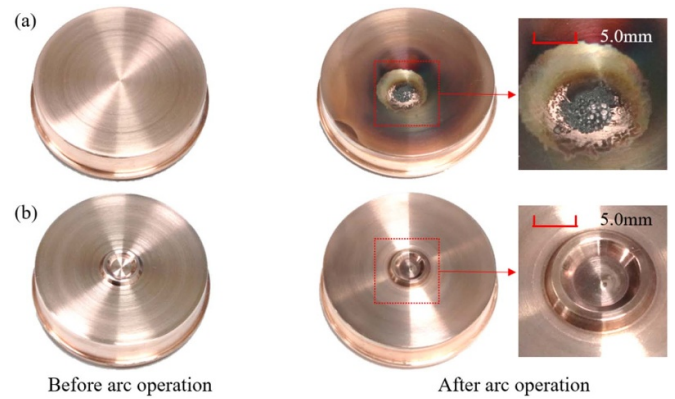


**Figure 9.** Photographs of anode surface before and after 1 h of arc operation; (a) planar anode. (b) annular boss anode.

The main advantage of diffuse arc attachment compared to constricted attachment is that it can reduce the current and heat flux density on the anode surface, thus reducing the heat transfer from the arc to the anode and preventing the occurrence of anode ablation. To test the effect of the annular boss anode on heat transfer to the arc anode, we operated the annular boss and planar anodes under the same conditions for one hour with an electrode separation of 30 mm. Figure 9 shows photos of the anode surface state before and after the experiment. The previous figures and analysis showed that the arc is attached to the surface of the planar anode in a constricted mode for a long electrode distance, and the current and heat flow density at the arc attachment region is relatively high. As a consequence, obvious ablation points are observed after arc operation. However, for the annular boss anode, since the arc anode attachment mode is diffuse under the same operating conditions, the anode surface remains in good condition with no obvious signs of ablation.

#### 4. Conclusions

In conclusion, this letter proposes a novel method to adjust the arc anode attachment mode by changing the anode surface structure. The experimental results show that with increasing

electrode separation, the arc attachment mode on the surface of the planar anode gradually changes from diffuse to constricted. For the annular boss anode, the arc anode attachment mode remains diffuse. By analyzing the electric field distribution between the electrodes, it was found that the annular boss on the surface of the anode enhances the local electric field strength due to the large curvature of the annular boss edges, which drives the arc to be evenly dispersed on the annular boss and plays an important role in adjusting the arc anode attachment mode. The ‘M-shaped’ electric field strength distribution above the annular boss anode indicates that the boss edges have a larger effect on enhancing the electric field strength than the flat part. It is possible to increase the electric field strength further by increasing the boss height and the sharp edge angle, which will make possible optimization of the boss geometry in future work. Subsequent work will focus on adjusting the anode structure to improve the anode attachment characteristics of molecular gas arcs, for which the heat flux to the anode and the consequent likelihood of damage are typically larger.

### Data availability statement

All data that support the findings of this study are included within the article (and any supplementary files).

### Acknowledgments

This work was supported by the National Natural Science Foundation of China (Grant Nos. 11735004, 12005010).

### ORCID iDs

Anthony B Murphy  <https://orcid.org/0000-0002-2820-2304>

Hai-Xing Wang  <https://orcid.org/0000-0001-7426-0946>

### References

- [1] Murphy A B and Uhrlandt D 2018 Foundations of high-pressure thermal plasmas *Plasma Sources Sci. Technol.* **27** 063001
- [2] Heberlein J V R, Mentel J and Pfender E 2010 The anode region of electric arcs: a survey *J. Phys. D: Appl. Phys.* **43** 023001
- [3] Sanders N A, Etemadi K, Hsu K C and Pfender E 1982 Studies of the anode region of a high-intensity argon arc *J. Appl. Phys.* **53** 4136–45
- [4] Chen D M and Pfender E 1980 Modeling of the anode contraction region of high intensity arcs *IEEE Trans. Plasma Sci.* **8** 252–9
- [5] Chazelas C, Trelles J P and Vardelle A 2017 The main issues to address in modeling plasma spray torch operation *J. Therm. Spray Technol.* **26** 3–11
- [6] Yang G and Heberlein J V R 2007 Anode attachment modes and their formation in a high intensity argon arc *Plasma Sources Sci. Technol.* **16** 529–42
- [7] Sun S R, Wang H X and Zhu T 2020 Numerical analysis of chemical reaction processes in different anode attachments of a high intensity argon arc *Contrib. Plasma Phys.* **60** 1–11
- [8] Sun S R, Wang H X, Zhu T and Murphy A B 2020 Chemical non-equilibrium simulation of anode attachment of an argon transferred arc *Plasma Chem. Plasma Process.* **40** 261–82
- [9] Mentel J and Heberlein J V R 2010 The anode region of low current arcs in high intensity discharge lamps *J. Phys. D: Appl. Phys.* **43** 023002
- [10] Jenista J, Heberlein J V R and Pfender E 1997 Numerical model of the anode region of high-current electric arcs *IEEE Trans. Plasma Sci.* **25** 883–90
- [11] Dinulescu H A and Pfender E 1980 Analysis of the anode boundary layer of high intensity arcs *J. Appl. Phys.* **51** 3149–57
- [12] Zhu T, Wang H X, Sun S R, Geng J and Shen Y 2019 Numerical simulation of constricted and diffusive arc–anode attachments in wall-stabilized transferred argon arcs *Plasma Sci. Technol.* **21** 57–66
- [13] Xia W, Li L, Zhao Y, Ma Q, Du B, Chen Q and Cheng L 2006 Dynamics of large-scale magnetically rotating arc plasmas *Appl. Phys. Lett.* **88** 211501
- [14] Pan W, Chen L, Meng X, Zhang Y and Wu C 2016 Sufficiently diffused attachment of nitrogen arc by gasdynamic action *Theor. Appl. Mech. Lett.* **6** 293–6
- [15] Sun J, Sun S, Wang H, Niu C and Zhu T 2020 Comparative analysis of the arc characteristics inside the converging-diverging and cylindrical plasma torches *Plasma Sci. Technol.* **22** 81–91
- [16] Vardelle A *et al* 2016 The 2016 thermal spray roadmap *J. Therm. Spray Technol.* **25** 1376–440
- [17] Anders A 2008 *Cathodic Arc* (Berlin: Springer)
- [18] Schmoll R 1998 Analysis of the interaction of cathode micro-protrusions with low-temperature plasmas *J. Phys. D: Appl. Phys.* **31** 1841–51
- [19] Beilis I I 2006 Non steady cathode spot operation at a microprotrusion in a vacuum arc *Int. Symp. on Discharges and Electrical Insulation in Vacuum, Matsue, Japan* vol 1 pp 388–91
- [20] Boxman R L, Martin P J and Sanders D M 1996 *Hand Book of Vacuum Arc Science and Technology: Fundamentals and Applications* (NJ: Noyes Publications)
- [21] Guo H, Li P, Li H P, Ge N and Bao C Y 2016 *In situ* measurement of the two-dimensional temperature field of a dual-jet direct-current arc plasma *Rev. Sci. Instrum.* **87** 033502
- [22] Ge N, Wu G Q, Li H P, Wang Z and Bao C Y 2011 Evaluation of the two-dimensional temperature field and instability of a dual-jet dc arc plasma based on the image chain coding technique *IEEE Trans. Plasma Sci.* **39** 2884–5
- [23] Wang Z, Wu G Q, Ge N, Li H P and Bao C Y 2010 Volt-ampere and thermal features of a direct-current dual-jet plasma generator with a cold gas injection *IEEE Trans. Plasma Sci.* **38** 2906–13